Learning from a Complementary-label Source Domain: Theory and Algorithms

Yiyang Zhang†, Feng Liu†, *Member, IEEE*, Zhen Fang†,
Bo Yuan, *Senior Member, IEEE*, Guangquan Zhang, and Jie Lu*, *Fellow, IEEE*

***Abstract*—In *unsupervised domain adaptation* (UDA), a classifier for the target domain is trained with massive *true-label* data from the source domain and unlabeled data from the target domain. However, collecting true-label data in the source domain can be expensive and sometimes impractical. Compared to the true label, a complementary label specifies a class that a pattern does not belong to, and hence collecting complementary labels would be less laborious than collecting true labels. In this paper, we propose a novel setting where the source domain is composed of *complementary-label* data, and a theoretical bound of this setting is provided. We consider two cases of this setting: one is that the source domain only contains complementary-label data (completely complementary unsupervised domain adaptation, CC-UDA), and the other is that the source domain has plenty of complementary-label data and a small amount of true-label data (partly complementary unsupervised domain adaptation, PC-UDA). To this end, a *complementary label adversarial network* (CLARINET) is proposed to solve CC-UDA and PC-UDA problems. CLARINET maintains two deep networks simultaneously, with one focusing on classifying the complementary-label source data and the other taking care of the source-to-target distributional adaptation. Experiments show that CLARINET significantly outperforms a series of competent baselines on handwritten digits recognition and objects recognition tasks.**

***Index Terms*—Transfer Learning; Domain Adaptation; Deep Learning; Complementary Labels**

I. Introduction

DOMAIN Adaptation (DA) aims to train a target-domain classifier with data in source and target domains [1], [2], [3], [4]. Based on the availability of data in the target domain (e.g., fully-labeled, partially-labeled and unlabeled), DA is divided into three categories: supervised DA [5], [6], [7], semi-supervised DA [8], [9], [10] and *unsupervised DA* (UDA) [11], [12], [13]. In practical applications, UDA is more challenging and promising than the other two as the labeled target domain data are not needed [14], [15], [16].

UDA methods train a target-domain classifier with massive true-label data from the source domain (true-label source data) and unlabeled data from the target domain (unlabeled target data). Existing works in the literature can be roughly categorised into the following three groups: integral-probability-metrics based UDA [17], [18]; adversarial-training based UDA [19], [20]; and causality-based UDA [21], [22]. Since adversarial-training based UDA methods extract better domain-invariant representations via deep networks, they usually have good target-domain accuracy [23].

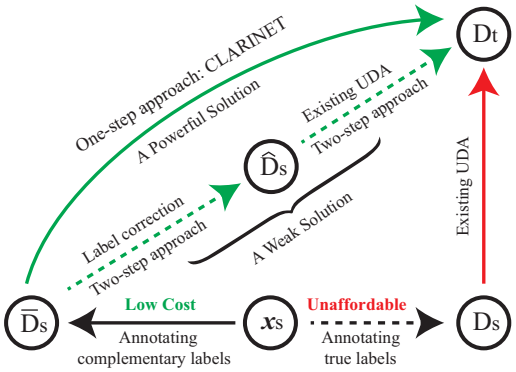

Fig. 1: Complementary-label based UDA. The red line denotes that UDA methods transfer knowledge from D_s (true-label source data) to D_t (unlabeled target data). However, acquiring true-label source data is *costly* and *unaffordable* (black dash line, $\mathbf{x}_s \to D_s$, $\mathbf{x}_s$ means unlabeled source data). This brings complementary-label based UDA, namely transferring knowledge from $\overline{D}_s$ (complementary-label source data) to D_t. It is much less costly to collect complementary-label source data (black line, required by our setting) than collecting the true-label one (black dash line, required by UDA). To handle complementary-label based UDA, a weak solution is a two-step approach (green dash line), which sequentially combines complementary-label learning methods ($\overline{D}_s \to \hat{D}_s$, label correction) and existing UDA methods ($\hat{D}_s \to D_t$). This paper proposes a one-step approach called *complementary label adversarial network* (CLARINET, green line, $\overline{D}_s \to D_t$ directly).

However, the success of UDA still highly relies on the scale of true-label source data (black dash line in Figure 1). Namely, the target-domain accuracy of a UDA method, e.g., *conditional domain adversarial network* (CDAN) [20], decays when the scale of true-label source data decreases and we prove this phenomenon in the experiment section. Hence, massive true-label source data are inevitably required by UDA methods, which is very expensive and even prohibitive.

While determining the correct label from many candidates is laborious, choosing one of the incorrect labels (i.e., complementary labels), e.g., labeling a cat as "Not Monkey" (as shown in Figure 2), would be much easier and quicker, thus less costly, especially when we have many candidates [24]. Comparing with picking out the true label from many candidates, judging the correctness of a label randomly given by the system is much easier. Besides, it is impossible to find

Yiyang Zhang is with the Australian Artificial Intelligence Institute, University of Technology Sydney, Sydney, NSW, 2007, Australia, and Shenzhen International Graduate School, Tsinghua University, Shenzhen, P.R. China (e-mail: zhangyiy18@mails.tsinghua.edu.cn).

Feng Liu, Zhen Fang, Guangquan Zhang, and Jie Lu are with the Australian Artificial Intelligence Institute, University of Technology Sydney, Sydney, NSW, 2007, Australia (e-mail: feng.liu@uts.edu.au; zhen.fang@student.uts.edu.au; jie.lu@uts.edu.au; guangquan.zhang@uts.edu.au).

Bo Yuan is with Shenzhen International Graduate School, Tsinghua University, Shenzhen, P.R. China (e-mail: boyuan@ieee.org).

†Equal contribution. *Corresponding author.

crowd-workers who have the knowledge of all classes in some areas (e.g., translation), and it is hard to collect true labels in traditional way in this case. However, we can choose a class randomly, and then assign the unlabeled sample to the expert of that randomly chosen class. It would be feasible to judge the correctness of the chosen label.

In addition to reducing costs, complementary labels also could help ensure data privacy. Even when we can collect true labels, it is sometimes better to convert them to complementary labels on purpose. This way, when companies suffer from data leakage, they won't reveal the true label of customers. In addition, such business strategy might make customers who do not want their data to be saved in databases more comfortable.

This brings us a novel setting, complementary-label based UDA, which aims to transfer knowledge from complementary-label source data to unlabeled target data (Figure 1). Compared to ordinary UDA, we can greatly save the labeling cost by annotating complementary labels in the source domain rather than annotating true labels [24], [25]. Please note, existing UDA methods cannot handle the complementary-label based UDA, as they require source data with complete true labels [12], [13] or at least 20% true-label source data [26], [27]. [1]

In the previous work [28], we consider using completely complementary-label data in the source domain, while actually we could also get a small amount of true labels when collecting complementary labels [24]. Therefore, the previous work was flawed as it did not make good use of the existing true-label data. Furthermore, experiments were conducted only on some digit datasets and a thorough learning bound was not provided. Aiming at these defects, in this work, we consider a generalized and completed version of the complementary-label based UDA problem setting.

A straightforward but weak solution to complementary-label based UDA is a two-step approach, which sequentially combines *complementary-label learning* methods and existing UDA methods (green dash line in Figure 1)[2]. Complementary-label learning methods are used to assign pseudo labels for complementary-label source data. Then, we can train a target-domain classifier with pseudo-label source data and unlabeled target data using existing UDA methods. Nevertheless, pseudo-label source data contain noise, which may cause poor domain-adaptation performance of this two-step approach [26].

Therefore, we propose a powerful one-step solution, *complementary label adversarial network* (CLARINET). It maintains two deep networks trained by adversarial way simultaneously, where one can accurately classify complementary-label source data, and the other can discriminate source and target domains. Since Long et al. [20] and Song et al. [29] have shown that the multimodal structures of distributions can only be captured sufficiently by the cross-covariance dependency between the features and classes (i.e., true labels), we set the input of domain discriminator D as the outer product of feature representation (e.g., $\boldsymbol{g}_s$ in Figure 3) and scattered classifier prediction (e.g., $\boldsymbol{T}(\boldsymbol{f}_s)$ in Figure 3).

Due to the nature of complementary-label classification, the predicted probability of each class (i.e., each element of $\boldsymbol{f}_s$, Figure 3) is relatively close. According to [29], this kind of predicted probabilities could not provide sufficient information to capture the multimodal structure of distributions. To fix it, we add a sharpening function T to make the predicted probabilities more scattered (i.e., $\boldsymbol{T}(\boldsymbol{f}_s)$, Figure 3) than previous ones (i.e., $\boldsymbol{f}_s$, Figure 3). By doing so, the scattered classifier predictions can better indicate their choice. In this way, we can take full advantage of classifier predictions and effectively align distributions of two domains. Our ablation study (see Table III) verifies that the sharpening function T indeed helps improve the target-domain accuracy.

We conduct experiments on 7 complementary-label based UDA tasks and compare CLARINET with a series of competent baselines. Empirical results demonstrated that CLARINET effectively transfers knowledge from complementary-label source data to unlabeled target data and is superior to all baselines. We also show that the target-domain accuracy of CLARINET will increase if a small amount of true-label source data are available. To make up for the defects of previous conference paper [28], the main contributions of this paper are summarized as follows.

1) We present a generalized version of the complementary-label based UDA. This paper considers two cases of complementary-label based UDA: one is that the source domain only contains complementary-label data (completely complementary unsupervised domain adaptation, CC-UDA), and the other is that the source domain also contains a small amount of true-label data (partly complementary unsupervised domain adaptation, PC-UDA).
2) We provide a thorough theoretical analysis of the expected target-domain risk of our approach, presenting a learning bound of complementary-label based UDA.
3) Apart from the handwritten digit datasets, we also conduct experiments on more complex image datasets, proving the applicability of complementary-label based UDA.

This paper is organized as follows. Section II reviews the works related to domain adaptation, complementary-label learning, and low-cost unsupervised domain adaptation. Section III introduces the problem setting and proves a learning bound of this setting. Section IV introduces a straightforward but weak two-step approach to complementary-label based UDA. The proposed powerful one-step solution is shown in Section V. Experimental results and analyses are provided in Section VI. Finally, Section VII concludes this paper.

II. Related Works

In this section, we discuss previous works that are most related to our work, and highlight our differences from them. We mainly review some related works about domain adaptation, complementary-label learning and low-cost unsupervised domain adaptation.

[1] In [26], [27], they consider the case where the sample in the source domain is noisy. With only 20% true labels, some of the baseline models achieve very low target domain accuracy. Therefore, Liu et al. believe that at least 20% true-label source data are needed to realize domain adaptation.

[2] We implement this two-step approach and take it as a baseline.

Fig. 2: True label (top) versus complementary label (bottom).

A. Domain Adaptation

Domain adaptation generalizes a learner across different domains by matching the distributions of source and target domains. It has wide applications in computer vision [30], [31], [32] and natural language processing [33], [34], etc. Previous domain adaptation methods in the shallow regime either try to bridge the source and target domains by learning invariant feature representations or estimating instance importance using labeled source data and unlabeled target data [35], [36]. Later, it is confirmed that deep learning methods formed by the composition of multiple non-linear transformations yield abstract and ultimately useful representations [37]. Besides, the learned deep representations to some extent are general and are transferable to similar tasks [38]. Hence, deep neural networks have been explored for domain adaptation.

Concurrently, multiple methods of matching the feature distributions in the source and the target domains have been proposed for unsupervised domain adaptation. The first category learns domain invariant features by minimizing a distance between distributions, such as *maximum mean discrepancy* (MMD) [39]. In *deep adaptation network* (DAN) [17], Long et al. minimize the marginal distributions of two domains by *multi-kernel MMD* (MK-MMD) metric. An alternative way of learning domain invariant features in UDA is inspired by the *generative adversarial networks* (GANs). By confusing a domain classifier (or discriminator), the deep networks can explore non-discriminative representations. The adversarial-training based UDA methods always try to play a two-player minimax game. *Domain-adversarial neural network* (DANN) [40] employs a gradient reversal layer to realize the minimax optimation. In [20], they propose CDAN, which conditions the models on discriminative information conveyed in the classifier predictions. Some works study the UDA problem from a causal point of view where they consider the label Y is the cause for feature representation X. In [21], Gong et al. aim to extract conditional transferable components whose conditional distribution is invariant after proper transformations.

However, the aforementioned methods all based on the true-label source data, which require high labeling costs. In our work, we propose a new setting by using complementary-label source data instead of true-label source data, which significantly saves the labeling cost.

B. Complementary-label Learning

Complementary-label learning (shown in Figure 2) is one type of weak supervision learning approaches, which is first proposed by Ishida et al. [24]. They give theoretical analysis with a statistical consistency guarantee to show classification risk can be recovered only from complementary-label data. Nevertheless, they require the complementary label must be chosen in an unbiased way and allow only one-versus-all and pairwise comparison multi-class loss functions with certain non-convex binary losses. Namely softmax cross-entropy loss, which is the most popular loss used in deep learning, could not be used to solve the problem.

Later, Yu et al. [25] extend the problem setting to where complementary label could be chosen in the biased way with the assumption that a small set of easily distinguishable true-label data are available in practice. In their point of view, due to humans are biased towards their own experience, it is unrealistic to guarantee the complementary label is chosen in an unbiased way. For example, if an annotator is more familiar with one class than with another, she is more likely to employ the more familiar one as a complementary label. They solve the problem by employing the forward loss correction technique to adjust the learning objective, but limiting the loss function to softmax cross-entropy loss. They theoretically ensure that the classifier learned with complementary labels converges to the optimal one learned with true labels.

Recently, Ishida et al. propose a new unbiased risk estimator [41] under the unbiased label chosen assumption. They make any loss functions available for use and have no implicit assumptions on the classifier, namely the estimator could be used for arbitrary models and losses, including softmax cross-entropy loss. They further investigate correction schemes to make complementary label learning practical and demonstrate the performance. Thus in our paper, we take advantage of this estimator for the source domain classification and generalize it to the unsupervised domain adaptation field.

C. Low-cost UDA

The UDA with low cost source data has recently attracted much attention. For instance, in [26], they consider the situation where the labeled data in the source domain come from amateur annotators or the Internet [42], [43]. As in the wild, acquiring a large amount of perfectly clean labeled data in the source domain is high-cost and sometimes impossible. They name the problem as *wildly unsupervised domain adaptation* (WUDA), which aims to transfer knowledge from noisy labeled data in the source domain to unlabeled target data. They show that WUDA ruins all UDA methods if taking no care of label noise in the source domain and propose a Butterfly framework, a powerful and efficient solution to WUDA.

Long et al. consider the weakly-supervised domain adaptation, where the source domain with noises in labels, features,

or both could be tolerated [27]. Label noise refers to incorrect labels of images due to errors in manual annotation, and feature noise refers to low-quality pixels of images, which may come from blur, overlap, occlusion, or corruption etc. They present a *transferable curriculum learning* (TCL) approach, extending from curriculum learning and adversarial learning. The TCL model aims to be robust to both sample noises and distribution shift by employing a curriculum which could tell whether a sample is easy and transferable.

In [28], we consider another way to save the labeling cost by using completely complementary-label data in the source domain and prove that distributional adaptation can be effectively realized from complementary-label source data to unlabeled target data. In this paper, we consider two cases of using complementary-label data in the source domain and prove that we could use a small amount of true-label data to improve the transfer result. Besides, as shown in [24], we can obtain true-label data and complementary-label data simultaneously, so that getting a small amount of true-label data is guaranteed to be low-cost. Furthermore, we provide an analysis of the expected target-domain risk of our approach. In the following sections, we will introduce the complementary-label based UDA and explain how to address such tasks.

III. Complementary-label based UDA

This section presents a novel problem setting, complementary-label based UDA, and prove a learning bound for it. Then, we show its benefits for DA field

A. Problem Setting

In complementary-label based UDA, we aim to realize distributional adaptation from complementary-label source data to unlabeled target data. We first consider the situation where there are only complementary-label data in the source domain, namely *completely complementary UDA* (CC-UDA). Let $\mathcal{X} \subset \mathbb{R}^d$ be a feature (input) space and $\mathcal{Y} := \{\mathbf{y}_1, ..., \mathbf{y}_c, ..., \mathbf{y}_K\}$ be a label (output) space, where $\mathbf{y}_c$ is the one-hot vector for label c. A *domain* is defined as follows.

Definition 1 (Domains for CC-UDA)**.** *Given random variables $X_s, X_t \in \mathcal{X}$, $Y_s, \overline{Y}_s, Y_t \in \mathcal{Y}$, the source and target domains are joint distributions $P(X_s, \overline{Y}_s)$ and $P(X_t, Y_t)$, where the joint distributions $P(X_s, Y_s) \neq P(X_t, Y_t)$ and $P(\overline{Y}_s = \mathbf{y}_c | Y_s = \mathbf{y}_c) = 0$ for all $\mathbf{y}_c \in \mathcal{Y}$.*

Then, we propose CC-UDA problem as follows.

Problem 1 (CC-UDA)**.** *Given independent and identically distributed (i.i.d.) labeled samples $\overline{D}_s = \{(\mathbf{x}_s^i, \overline{\mathbf{y}}_s^i)\}_{i=1}^{\overline{n}_s}$ drawn from the source domain $P(X_s, \overline{Y}_s)$ and i.i.d. unlabeled samples $D_t = \{\mathbf{x}_t^i\}_{i=1}^{n_t}$ drawn from the target marginal distribution $P(X_t)$, the aim of CC-UDA is to train a classifier $F_t : \mathcal{X} \to \mathcal{Y}$ with $\overline{D}_s$ and D_t such that F_t can accurately classify target data drawn from $P(X_t)$.*

It is clear that it is impossible to design a suitable learning procedure without any assumptions on $P(X_s, \overline{Y}_s)$. In this paper, we use the assumption for unbiased complementary-label learning proposed by [24], [41]:

$$P(\overline{Y}_s = \mathbf{y}_k | X_s) = \frac{1}{K-1} \sum_{c=1, c\neq k}^{K} P(Y_s = \mathbf{y}_c | X_s), \quad (1)$$

for all $k, c \in \{1, ..., K\}$ and $c \neq k$. This unbiased assumption indicates that the selection of complementary labels for samples is with equal probability.

Ishida et al. [24] propose an efficient way to collect labels through crowdsourcing: we choose one of the classes randomly and ask crowd-workers whether a pattern belongs to the chosen class or not. Then the chosen class is treated as true label if the answer is yes; otherwise, the chosen class is regarded as complementary label. Such a yes/no question is much easier and quicker than selecting the correct class from the list of all candidate classes, which sometimes could even be impossible. In addition, we could guarantee that the data gotten through this way are under unbiased assumption in Eq. (1).

As we can obtain true-label data and complementary-label data simultaneously, we also consider the problem that the source domain contains a few true-label data. We name this problem as *partly complementary UDA* (PC-UDA).

Problem 2 (PC-UDA)**.** *Given i.i.d labeled samples $\overline{D}_s = \{(\mathbf{x}_s^i, \overline{\mathbf{y}}_s^i)\}_{i=1}^{\overline{n}_s}$ drawn from the domain $P(X_s, \overline{Y}_s)$, $D_s = \{(\mathbf{x}_s^i, \mathbf{y}_s^i)\}_{i=\overline{n}_s+1}^{\overline{n}_s+n_s}$ drawn from the domain $P(X_s, Y_s)$, and i.i.d unlabeled samples $D_t = \{\mathbf{x}_t^i\}_{i=1}^{n_t}$ drawn from the target marginal distribution $P(X_t)$, the aim is to find a target classifier $F_t : \mathcal{X} \to \mathcal{Y}$ such that F_t classifies target samples into the correct classes.*

It is actually a more common situation to have a small amount of true-label data. If we leverage both kinds of labeled data properly, we could obtain a more accurate classifier. Ishida et al. [24] have demonstrated the usefulness of combining true-label and complementary-label data in classification problem. We will further show that in unsupervised domain adaptation field, we could also use both true-label and complementary-label source data to realize knowledge transfer and utilize the true-label data to improve the result.

B. Learning Bound of complementary-label based UDA

A learning bound of complementary-label based UDA is presented in this subsection. We could prove that we can limit the risk in the target domain. Practitioner may safely skip it.

If given a feature transformation:

$$\begin{aligned} G : \mathcal{X} &\to \mathcal{X}_G := G(\mathcal{X}) \\ \mathbf{x} &\to \mathbf{x}_G := G(\mathbf{x}), \end{aligned} \quad (2)$$

then the induced distributions related to P_{X_s} and P_{X_t} are

$$\begin{aligned} G_{\#} P_{X_s} &:= P(G(X_s)); \\ G_{\#} P_{X_t} &:= P(G(X_t)). \end{aligned} \quad (3)$$

Following the notations in [44], consider a multi-class classification task with a *hypothesis space* $\mathcal{H}_G$ of the classifiers

$$\begin{aligned} F : \ \mathcal{X}_G &\to \mathcal{Y} \\ \mathbf{x} &\to [C_1(\mathbf{x}), ..., C_K(\mathbf{x})]^T. \end{aligned} \quad (4)$$

Let

$$\begin{aligned} \ell : \mathbb{R}^K \times \mathbb{R}^K &\to \mathbb{R}_{\geq 0} \\ (\mathbf{y}, \tilde{\mathbf{y}}) &\to \ell(\mathbf{y}, \tilde{\mathbf{y}}), \end{aligned} \quad (5)$$

be the loss function. For convenience, we also require ℓ satisfying the following conditions in theoretical part:
1. ℓ is symmetric and satisfies triangle inequality;
2. $\ell(\mathbf{y},\tilde{\mathbf{y}})=0$ iff $\mathbf{y}=\tilde{\mathbf{y}}$;
3. $\ell(\mathbf{y},\tilde{\mathbf{y}})\equiv 1$ if $\mathbf{y}\neq\tilde{\mathbf{y}}$ and $\mathbf{y},\tilde{\mathbf{y}}$ are one-hot vectors.

We can check many losses satisfying the above conditions, such as 0-1 loss $1_{\mathbf{y}\neq\tilde{\mathbf{y}}}$ and ℓ_2 loss $\frac{1}{2}\|\mathbf{y}-\tilde{\mathbf{y}}\|_2^2$. The complementary risk for $F\circ G$ with respect to ℓ over $P(X_s,\overline{Y}_s)$ is

$$L_{\overline{s}}(F\circ G)=\mathbb{E}\ell(F\circ G(X_s),\overline{Y}_s).$$

The risks for the decision function $F\circ G$ with respect to loss ℓ over implicit distribution $P(X_s,Y_s),P(X_t,Y_t)$ are:

$$L_s(F\circ G)=\mathbb{E}\ell(F\circ G(X_s),Y_s),$$
$$L_t(F\circ G)=\mathbb{E}\ell(F\circ G(X_t),Y_t).$$

In this paper, we propose a tighter distance named tensor discrepancy distance. The tensor discrepancy distance can future math the pseudo conditional distributions.

We consider the following tensor mapping:

$$\begin{aligned}\otimes_F:\mathcal{X}_G&\to\mathcal{X}_G\otimes\mathcal{Y}_t\\ \mathbf{x}_G&\to\mathbf{x}_G\otimes F(\mathbf{x}_G).\end{aligned}\tag{6}$$

Then we induce two important distributions:

$$\begin{aligned}\otimes_{F\#}P_{X_s}&:=P(\otimes_F(G(X_s)));\\ \otimes_{F\#}P_{X_t}&:=P(\otimes_F(G(X_t))).\end{aligned}\tag{7}$$

Using $\mathcal{H}_G$, we reconstruct a new hypothetical set:

$$\Delta_{F,G}:=\{\delta_{\overline{F}}:\mathcal{X}_G\otimes\mathcal{Y}^t\to\mathbb{R}:\overline{F}\in\mathcal{H}_G\},\tag{8}$$

where $\delta_{\overline{F}}(\mathbf{x}_G\otimes\mathbf{y})=|\otimes_F(\mathbf{x}_G)-\otimes_{\overline{F}}(\mathbf{x}_G)|$. Then the distance between $\otimes_{F\#}P_{X_s}$ and $\otimes_{F\#}P_{X_t}$ is:

$$\begin{aligned}&d^{\ell}_{\Delta_{F,G}}(\otimes_{F\#}P_{X_s},\otimes_{F\#}P_{X_t})\\ &=\sup_{\delta\in\Delta_{F,G}}\Big|\mathop{\mathbb{E}}_{\mathbf{z}\sim\otimes_{F\#}P_{X_s}}\mathrm{sgn}\circ\delta(\mathbf{z})-\mathop{\mathbb{E}}_{\mathbf{z}\sim\otimes_{F\#}P_{X_t}}\mathrm{sgn}\circ\delta(\mathbf{z})\Big|,\end{aligned}\tag{9}$$

where sgn is the sign function.

It is easy to prove that under the conditions 1-3 for loss ℓ and for any $F\in\mathcal{H}_G$, we have

$$d^{\ell}_{\Delta_{F,G}}(\otimes_{F\#}P_{X_s},\otimes_{F\#}P_{X_t})\le d^{\ell}_{\mathcal{H}_G}(G_{\#}P_{X_s},G_{\#}P_{X_t}),\tag{10}$$

where $d^{\ell}_{\mathcal{H}_G}$ is the distribution discrepancy defined in [45], [46]. Then, we introduce our main theorem as follows.

Theorem 1. *Given a loss function ℓ satisfying conditions 1-3 and a hypothesis $\mathcal{H}_G\subset\{F:\mathcal{X}_G\to\mathcal{Y}\}$, then under unbiased assumption, for any $F\in\mathcal{H}_G$, we have*

$$L_t(F\circ G)\le\overline{L}_s(F\circ G)+\Lambda+d^{\ell}_{\Delta_{F,G}}(\otimes_{F\#}P_{X_s},\otimes_{F\#}P_{X_t}),$$

where $\overline{L}_s(F\circ G):=\sum_{k=1}^{K}\int_{\mathcal{X}}\ell(F\circ G(\mathbf{x}),k)\mathrm{d}P_{X_s}-(K-1)L_{\overline{s}}(F\circ G)$, P_{X_s},P_{X_t} are source and target marginal distributions, $\Lambda=\min_{F\in\mathcal{H}_G}\ R_s(F\circ G)+R_t(F\circ G)$.

Proof. Firstly, we prove that $L_s(F\circ G)=\overline{L}_s(F\circ G)$. To prove it, we investigate the connection between $L_s(F\circ G)$ and $L_{\overline{s}}(F\circ G)$ under unbiased assumption in Eq. (1). Given $K\times K$ matrix Q whose diagonal elements are 0 and other elements are $1/K$, we represent the unbiased assumption by

$$\overline{\boldsymbol{\eta}}=Q\boldsymbol{\eta},\tag{11}$$

where $\overline{\boldsymbol{\eta}}=[P(\overline{Y}_s=\mathbf{y}_1|X_s),...,P(\overline{Y}_s=\mathbf{y}_K|X_s)]^T$ and $\boldsymbol{\eta}=[P(Y_s=\mathbf{y}_1|X_s),...,P(Y_s=\mathbf{y}_K|X_s)]^T$. Note that Q has inverse matrix Q^{-1} whose diagonal elements are $-(K-2)$ and other elements are 1. Thus, we have that

$$Q^{-1}\overline{\boldsymbol{\eta}}=\boldsymbol{\eta}.\tag{12}$$

According to Eq. (12), we have $P(Y_s=\mathbf{y}_k|X_s)=1-(K-1)P(\overline{Y}_s=\mathbf{y}_k|X_s)$, which implies that

$$\begin{aligned}L_s(F\circ G)=&\sum_{k=1}^{K}\int_{\mathcal{X}}\ell(F\circ G(\mathbf{x}),k)\mathrm{d}P_{X_s}\\ &-(K-1)L_{\overline{s}}(F\circ G).\end{aligned}\tag{13}$$

Hence, $L_s(F\circ G)=\overline{L}_s(F\circ G)$. The empirical form of Eq. (13) is known as complementary-label loss (see Eq. (20)).

Next we will prove that

$$L_t(F\circ G)-L_s(F\circ G)\le\Lambda+d^{\ell}_{\Delta_{F,G}}(\otimes_{F\#}P_{X_s},\otimes_{F\#}P_{X_t}).$$

As if it is true, combined with $L_s(F\circ G)=\overline{L}_s(F\circ G)$, we could easily prove the theorem. It is clearly that

$$\begin{aligned}&L_t(F\circ G)-L_s(F\circ G)\\ =&\int_{\mathcal{X}\times\mathcal{Y}_t}\ell(F\circ G(\mathbf{x}),\mathbf{y})\mathrm{d}P_{X_tY_t}-\int_{\mathcal{X}\times\mathcal{Y}_s}\ell(F\circ G(\mathbf{x}),\mathbf{y})\mathrm{d}P_{X_sY_s}\\ \le&\ L_t(\widetilde{F}\circ G)+\int_{\mathcal{X}\times\mathcal{Y}^t}\ell(F\circ G(\mathbf{x}),\widetilde{F}\circ G(\mathbf{x}))\mathrm{d}P_{X_tY_t}\\ &+L_s(\widetilde{F}\circ G)-\int_{\mathcal{X}\times\mathcal{Y}_s}\ell(F\circ G(\mathbf{x}),\widetilde{F}\circ G(\mathbf{x}))\mathrm{d}P_{X_sY_s},\end{aligned}\tag{14}$$

where $\widetilde{F}$ is any function from $\mathcal{H}_G$. According to conditions 1-3, we have that

$$\begin{aligned}\mathop{\mathbb{E}}_{\mathbf{z}\sim\otimes_{F\#}P_{X_s}}\mathrm{sgn}\circ\delta_{\widetilde{F}}(\mathbf{z})&=\int\mathrm{sgn}\circ\delta_{\widetilde{F}}(\mathbf{z})\mathrm{d}\otimes_{F\#}P_{X_s}\\ &=\int_{\mathcal{X}}|F\circ G(\mathbf{x})-\widetilde{F}\circ G(\mathbf{x})|\mathrm{d}P_{X_s}\\ &=\int_{\mathcal{X}}\ell(F\circ G(\mathbf{x}),\widetilde{F}\circ G(\mathbf{x}))\mathrm{d}P_{X_s},\end{aligned}\tag{15}$$

similarly,

$$\mathop{\mathbb{E}}_{\mathbf{z}\sim\otimes_{F\#}P_{X_t}}\mathrm{sgn}\circ\delta_{\widetilde{F}}(\mathbf{z})=\int_{\mathcal{X}}\ell(F\circ G(\mathbf{x}),\widetilde{F}\circ G(\mathbf{x}))\mathrm{d}P_{X_t},\tag{16}$$

hence, according to the definition of Eq. (9), we have

$$\begin{aligned}&d^{\ell}_{\Delta_{F,G}}(\otimes_{F\#}P_{X_s},\otimes_{F\#}P_{X_t})\\ &=\sup_{\widetilde{F},G\in\Delta_{F,G}}\Big|\int_{\mathcal{X}}\ell(F\circ G(\mathbf{x}),\widetilde{F}\circ G(\mathbf{x}))\mathrm{d}P_{X_s}\\ &\qquad-\int_{\mathcal{X}}\ell(F\circ G(\mathbf{x}),\widetilde{F}\circ G(\mathbf{x}))\mathrm{d}P_{X_t}\Big|.\end{aligned}\tag{17}$$

Combining Eq. (14) and Eq. (17), we have

$$\begin{aligned}&L_t(F\circ G)-L_s(F\circ G)\\ \le&\ \min(L_t(\widetilde{F}\circ G)+L_s(\widetilde{F}\circ G))+d^{\ell}_{\Delta_{F,G}}(\otimes_{F\#}P_{X_s},\otimes_{F\#}P_{X_t})\\ =&\ \Lambda+d^{\ell}_{\Delta_{F,G}}(\otimes_{F\#}P_{X_s},\otimes_{F\#}P_{X_t}).\end{aligned}\tag{18}$$

Hence, we prove this theorem. □

C. Benefits for DA Field

Collecting true-label data is always expensive in the real world. Thus, learning from less expensive data [47], [48], [49], [50] has been extensively studied in machine learning field, including label-noise leaning [51], [52], [53], pairwise/triple-wise constraints learning [54], [55], [56], positive-unlabeled

learning [57], [58], [59], complementary-label learning [24], [41], [25] and so on. Among all these research directions, obtaining complementary labels is a cost-effective option. As described in the previous works mentioned above, compared with choosing the true class out of many candidate classes precisely, collecting complementary labels is obviously much easier and less costly. In addition, a classifier trained with complementary-label data is equivalent to a classifier trained with true-label data as shown in [41].

Actually in the field of domain adaptation, the high cost of true-label data is also an important issue. At present, the success of DA still highly relies on the scale of true-label source data, which is a critical bottleneck. Under low cost limitation, it is unrealistic to obtain enough true-label source data and thus cannot achieve a good distribution adaptation result. For the same cost, we can get multiple times more complementary-label data than the true-label data. In addition, the adaptation scenario is limited to some commonly used datasets, e.g., handwritten digit datasets, as they have sufficient true labels to support distributional adaptation. This fact makes it difficult to generalize domain adaptation to more real-world scenarios where it is needed. Thus if we can reduce the labeling cost in the source domain, for example, by using complementary-label data to replace true-label data (complementary-label based UDA), we can promote domain adaptation to more fields.

Due to existing UDA methods require at least 20% true-label source data [26], they cannot handle complementary-label based UDA problem. To address the problem, we introduce a two-step approach, straightforward but weak solution, and then propose a powerful one-step solution, CLARINET.

IV. Two-step Approach

To solve the problem that existing UDA methods cannot be applied to complementary-label based UDA problems directly, a straightforward way is to apply a two-step strategy. Namely, we could sequentially combine complementary-label learning methods and existing UDA methods. Algorithm 1 presents how we realize the two-step approach for CC-UDA tasks specifically. In the two-step approach, we first use the complementary-label learning algorithm to train a classifier on the complementary-label source data (line 1). Then, we take advantage of the classifier to assign pseudo labels for source domain data (line 2). Finally, we train the target-domain classifier with pseudo-label source data and unlabeled target data using existing UDA methods (line 3). In this way, we can transfer knowledge from the newly formed pseudo-label source data to unlabeled target data. As for PC-UDA tasks, we could combine the pseudo-label source data gotten following the first two steps and existing true-label source data together to train the target-domain classifier.

Nevertheless, the pseudo-label source data contain noise, as complementary-label learning algorithms cannot be trained to produce a completely accurate classifier. As the noise will bring poor domain-adaptation performance [26], the two-step approach is a suboptimal choice. To solve this problem, we consider implementing both complementary-label learning and unsupervised domain adaptation in a network. In this way, the network will always try to classify source domain data accurately during the adaptation procedure. Besides, we consider using entropy conditioning to make the transfer process mainly based on the classification results with high confidence, which can greatly eliminates the noise effect compared with the two-step approach. Therefore, we propose a powerful one-step solution to complementary-label based UDA, CLARINET.

Algorithm 1 Two-step Approach for CC-UDA Tasks

Input: $\overline{D}_s = \{(\mathbf{x}_s^i, \overline{\mathbf{y}}_s^i)\}_{i=1}^{\overline{n}_s}$, $D_t = \{\mathbf{x}_t^i\}_{i=1}^{n_t}$.
Output: the target-domain classifier.

1: **Train** a classifier C using $\overline{D}_s = \{(\mathbf{x}_s^i, \overline{\mathbf{y}}_s^i)\}_{i=1}^{\overline{n}_s}$ based on the complementary-label learning algorithm.
2: **Use** C to pseudo-label $\overline{D}_s = \{\mathbf{x}_s^i\}_{i=1}^{\overline{n}_s}$, namely generate pseudo-label source data $\hat{D}_s = \{(\mathbf{x}_s^i, \hat{\mathbf{y}}_s^i)\}_{i=1}^{\hat{n}_s}$.
3: **Apply** normal UDA methods on $\hat{D}_s = \{(\mathbf{x}_s^i, \hat{\mathbf{y}}_s^i)\}_{i=1}^{\hat{n}_s}$ and $D_t = \{\mathbf{x}_t^i\}_{i=1}^{n_t}$ to train a target-domain classifier.

V. CLARINET: Powerful One-step Approach

The proposed CLARINET (as shown in Figure 3) realizes distributional adaptation in an adversarial way, which mainly consists of feature extractor G, label predictor F and domain discriminator D. By working adversarially to domain discriminator D, feature extractor G encourages domain-invariant features to emerge. Label predictor F are trained to discriminate different classes based on such features.

In this section, we first introduce two losses used to train CLARINET, complementary-label loss and scattered conditional adversarial loss. Then the whole training procedure of CLARINET is presented. Finally, we show how to adjust CLARINET for PC-UDA tasks if a small amount of true-label source data are available.

A. Loss Function in CLARINET

In this subsection, we introduce how to compute the two losses mentioned above in CLARINET after obtaining mini-batch $\overline{d}_s$ from $\overline{D}_s$ and d_t from D_t.

1) Complementary-label Loss: It is designed to reduce the source classification error based on complementary-label data (the first part in the bound). We first divided $\overline{d}_s$ into K disjoint subsets according to the complementary labels in $\overline{d}_s$,

$$\overline{d}_s = \cup_{k=1}^{K} \overline{d}_{s,k},\ \overline{d}_{s,k} = \{(\mathbf{x}_k^i, \mathbf{y}_k)\}_{i=1}^{\overline{n}_{s,k}}, \tag{19}$$

where $\overline{d}_{s,k} \cap \overline{d}_{s,k'} = \varnothing$ if $k \neq k'$ and $\overline{n}_{s,k} = |\overline{d}_{s,k}|$. Then, following Eq. (13), the complementary-label loss on $\overline{d}_{s,k}$ is

$$\begin{aligned}\overline{L}_s(G, F, \overline{d}_{s,k}) = &-(K-1)\frac{\overline{\pi}_k}{\overline{n}_{s,k}} \sum_{i=1}^{\overline{n}_{s,k}} \ell(F \circ G(\mathbf{x}_k^i), \mathbf{y}_k) \\ &+ \sum_{j=1}^{K} \frac{\overline{\pi}_j}{\overline{n}_{s,j}} \sum_{l=1}^{\overline{n}_{s,j}} \ell(F \circ G(\mathbf{x}_j^l), \mathbf{y}_k),\end{aligned} \tag{20}$$

where ℓ can be any loss and we use the cross-entropy loss, $\overline{\pi}_k$ is the proportion of the samples complementary-labeled k. The total complementary-label loss on $\overline{d}_s$ is as follows.

$$\overline{L}_s(G, F, \overline{d}_s) = \sum_{k=1}^{K} \overline{L}_s(G, F, \overline{d}_{s,k}). \tag{21}$$

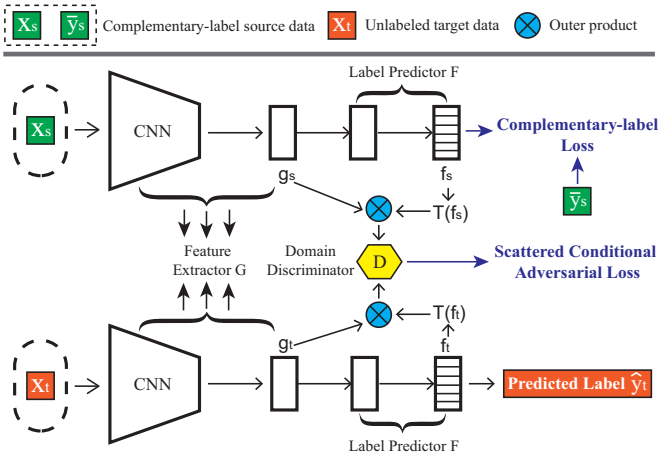

Fig. 3: Overview of the proposed *complementary label adversarial network* (CLARINET). It consists of feature extractor G, label predictor F and conditional domain discriminator D. g_s and g_t are outputs of G, representing extracted features of source and target data. f_s and f_t represent classifier predictions. T is a sharpening function, which we propose to scatter the classifier predictions. In Algorithm 2, we show how to use two losses mentioned in this figure to train CLARINET.

As shown in Section III-B, the complementary-label loss (i.e., Eq. (21)) is an unbiased estimator of the true-label-data risk. Namely, the minimizer of complementary-label loss agrees with the minimizer of the true-label-data risk with no constraints on the loss ℓ and model $F \circ G$ [41].

Remark 1. *Due to the negative part in $\overline{L}_s(G, F, \overline{d}_s)$, minimizing it directly will cause over-fitting [60]. To overcome this problem, we use a correctional way [41] to minimize $\overline{L}_s(G, F, \overline{d}_s)$ (lines 7-13 in Algorithm 2).*

2) Scattered Conditional Adversarial Loss: It is designed to reduce distribution discrepancy distance between two domains (the third part in the bound). Adversarial domain adaptation methods [19], [61] is inspired by *generative adversarial networks* (GANs) [62]. Normally, a domain discriminator is learned to distinguish the source domain and the target domain, while the label predictor learns transferable representations that are indistinguishable by the domain discriminator. Namely, the final classification decisions are made based on features that are both discriminative and invariant to the change of domains [19]. It is an efficient way to reduce distribution discrepancy distance between the marginal distributions.

However, when data distributions have complex multimodal structures, which is a real scenario due to the nature of multi-class classification, adapting only the feature representation is a challenge for adversarial networks. Namely, even the domain discriminator is confused, we could not confirm the two distributions are sufficiently similar [63].

According to [29], it is significant to capture multimodal structures of distributions using cross-covariance dependency between the features and classes (i.e., true labels). Since there are no true-label target data in UDA, CDAN adopts outer product of feature representations and classifier predictions (i.e., outputs of the softmax layer) as new features of two domains [20], which is inspired by *conditional generative adversarial networks* (CGANs) [64], [65]. The newly constructed features have shown great ability to discriminate source and target domains, since classifier predictions of true-label source data are dispersed, expressing the predicted goal clearly.

However, in the complementary-label classification mode, we observe that the predicted probability of each class (i.e., each element of $\boldsymbol{f_s}$ in Figure 3) is relatively close. Namely, it is hard to find significant predictive preference from the classifier predictions. According to [29], this kind of predictions cannot provide sufficient information to capture the multimodal structure of distributions. To fix it, we add a sharpening function T to scatter the predicted probability (the output of $\boldsymbol{f} = [f_1, ..., f_K]^T$ after softmax function, $\boldsymbol{f}$ could be $\boldsymbol{f_s}$ or $\boldsymbol{f_t}$ in Figure 3).

In [66], a common approach of adjusting the "temperature" of this categorical distribution is defined as follows,

$$T(\boldsymbol{f}) = \left[\frac{f_1^{\frac{1}{l}}}{\sum_{j=1}^{K} f_j^{\frac{1}{l}}}, ..., \frac{f_k^{\frac{1}{l}}}{\sum_{j=1}^{K} f_j^{\frac{1}{l}}}, ..., \frac{f_K^{\frac{1}{l}}}{\sum_{j=1}^{K} f_j^{\frac{1}{l}}} \right]^T. \quad (22)$$

As $l \to 0$, the output of $T(\boldsymbol{f})$ will approach a Dirac ("one-hot") distribution [67].

Then to prioritize the discriminator on those easy-to-transfer examples, following [20], we measure the uncertainty of the prediction for sample $\mathbf{x}$ by

$$H(G, F, \mathbf{x}) = -\sum_{k=1}^{K} T(f_k(\mathbf{x})) \log T(f_k(\mathbf{x})). \quad (23)$$

The small result implies that $T(f_k(\mathbf{x}))$ is close to 0 or 1, which could be regarded as the prediction is with high confidence due to the existing of the final softmax layer [68].

Thus the scattered conditional adversarial loss is as follows,

$$L_{adv}(G, F, D, \overline{d}_s, d_t) = -\frac{\sum_{\mathbf{x} \in \overline{d}_s[X]} \omega_{\overline{s}}(\mathbf{x}) \log(D(\boldsymbol{g}(\mathbf{x})))}{\sum_{\mathbf{x} \in \overline{d}_s[X]} \omega_{\overline{s}}(\mathbf{x})} - \frac{\sum_{\mathbf{x} \in d_t} \omega_t(\mathbf{x}) \log(1 - D(\boldsymbol{g}(\mathbf{x})))}{\sum_{\mathbf{x} \in d_t} \omega_t(\mathbf{x})}, \quad (24)$$

where $\omega_{\overline{s}}(\mathbf{x})$ and $\omega_t(\mathbf{x})$ are $1 + e^{-H(G,F,\mathbf{x})}$, $\boldsymbol{g}(\mathbf{x})$ is $G(\mathbf{x}) \otimes T(F \circ G(\mathbf{x}))$ and $\overline{d}_s[X]$ is the feature part of $\overline{d}_s$.

B. Training Procedures of CLARINET

Based on two losses proposed in Section V-A, in CLARINET, we try to solve the following optimization problem,

$$\begin{aligned} &\min_{G,F} \ \overline{L}_s(G, F, \overline{D}_s) - \lambda L_{adv}(G, F, D, \overline{D}_s, D_t), \\ &\min_{D} \ L_{adv}(G, F, D, \overline{D}_s, D_t), \end{aligned} \quad (25)$$

where D tries to distinguish the samples from different domains by minimizing L_{adv}, while $F \circ G$ wants to maximize the L_{adv} to make domains indistinguishable. To solve the minimax optimization problem in Eq. (25), we add a gradient reversal layer [19] between the domain discriminator and the classifier, which multiplies the gradient by a negative constant (-λ)

Algorithm 2 CLARINET for CC-UDA Tasks

Input: $\overline{D}_s = \{(\mathbf{x}_s^i, \overline{\mathbf{y}}_s^i)\}_{i=1}^{\overline{n}_s}$, $D_t = \{\mathbf{x}_t^i\}_{i=1}^{n_t}$.
Parameters: learning rate γ_1 and γ_2, epoch T_{max}, start epoch T_s, iteration N_{max}, class number K, tradeoff λ, network parameter $\theta_{F\circ G}$ and θ_D.
Output: the neural network $F\circ G$, namely the target domain classifier for D_t.

1: **Initialize** $\theta_{F\circ G}$ and θ_D;
2: **for** $t = 1, 2 \ldots\ldots T_{max}$ **do**
3: **Shuffle** the training set $\overline{D}_s$, D_t;
4: **for** $N = 1, 2 \ldots\ldots N_{max}$ **do**
5: **Fetch** mini-batch $\overline{d}_s$, d_t from $\overline{D}_s$, D_t;
6: **Divide** $\overline{d}_s$ into $\{\overline{d}_{s,k}\}_{k=1}^K$;
7: **Calculate** $\{\overline{L}_s(G, F, \overline{d}_{s,k})\}_{k=1}^K$ using Eq. (20), and $\overline{L}_s(G, F, \overline{d}_s)$ using Eq. (21);
8: **if** $\min_k\{\overline{L}_s(G, F, \overline{d}_{s,k})\}_{k=1}^K \geq 0$ **then**
9: **Update** $\theta_{F\circ G} = \theta_{F\circ G} - \gamma_1 \nabla \overline{L}_s(G, F, \overline{d}_s)$;
10: **else**
11: **Calculate** $\overline{L}_{neg} = \sum_{k=1}^K \min\{0, \overline{L}_s(G, F, \overline{d}_{s,k})\}$;
12: **Update** $\theta_{F\circ G} = \theta_{F\circ G} + \gamma_1 \nabla \overline{L}_{neg}$;
13: **end if**
14: **if** $t > T_s$ **then**
15: **Calculate** $L_{adv}(G, F, D, \overline{d}_s, d_t)$ using Eq. (24);
16: **Update** $\theta_D = \theta_D - \gamma_2 \nabla L_{adv}(G, F, D, \overline{d}_s, d_t)$;
17: **Update** $\theta_{F\circ G} = \theta_{F\circ G} + \gamma_2 \lambda \nabla L_{adv}(G, F, D, \overline{d}_s, d_t)$;
18: **end if**
19: **end for**
20: **end for**

Algorithm 3 CLARINET for PC-UDA Tasks

Input: $D_s = \{(\mathbf{x}_s^i, \mathbf{y}_s^i)\}_{i=1}^{n_s}$, $\overline{D}_s = \{(\mathbf{x}_s^i, \overline{\mathbf{y}}_s^i)\}_{i=1}^{\overline{n}_s}$, $D_t = \{\mathbf{x}_t^i\}_{i=1}^{n_t}$.
Parameters: learning rate γ_1 and γ_2, epoch T_{max}, start epoch T_s, iteration N_{max}, class number K, tradeoff λ and α, network parameter $\theta_{F\circ G}$ and θ_D.
Output: the neural network $F\circ G$, namely the target domain classifier for D_t.

1: **Initialize** $\theta_{F\circ G}$ and θ_D;
2: **for** $T = 1, 2 \ldots\ldots T_{max}$ **do**
3: **Shuffle** the training set D_s, $\overline{D}_s$, D_t;
4: **for** $N = 1, 2 \ldots\ldots N_{max}$ **do**
5: **Fetch** mini-batch d_s, $\overline{d}_s$, d_t from D_s, $\overline{D}_s$, D_t;
6: **Calculate** $L_s(G, F, d_s)$ using Eq. (26);
7: **Update** $\theta_{F\circ G} = \theta_{F\circ G} - \gamma_1 \alpha \nabla L_s(G, F, d_s)$;
8: **Divide** $\overline{d}_s$ into $\{\overline{d}_{s,k}\}_{k=1}^K$;
9: **Calculate** $\{\overline{L}_s(G, F, \overline{d}_{s,k})\}_{k=1}^K$ using Eq. (20), and $\overline{L}_s(G, F, \overline{d}_s)$ using Eq. (21);
10: **if** $\min_k\{\overline{L}_s(G, F, \overline{d}_{s,k})\}_{k=1}^K \geq 0$ **then**
11: **Update** $\theta_{F\circ G} = \theta_{F\circ G} - \gamma_1 (1-\alpha) \nabla \overline{L}_s(G, F, \overline{d}_s)$;
12: **else**
13: **Calculate** $\overline{L}_{neg} = \sum_{k=1}^K \min\{0, \overline{L}_s(G, F, \overline{d}_{s,k})\}$;
14: **Update** $\theta_{F\circ G} = \theta_{F\circ G} + \gamma_1 (1-\alpha) \nabla \overline{L}_{neg}$;
15: **end if**
16: **if** $T > T_s$ **then**
17: **Calculate** $L_{adv}(G, F, D, d_s, \overline{d}_s, d_t)$ using Eq. (28);
18: **Update** $\theta_D = \theta_D - \gamma_2 \nabla L_{adv}(G, F, D, d_s, \overline{d}_s, d_t)$;
19: **Update** $\theta_{F\circ G} += \gamma_2 \lambda \nabla L_{adv}(G, F, D, d_s, \overline{d}_s, d_t)$;
20: **end if**
21: **end for**
22: **end for**

during the back-propagation. λ is a hyper-parameter between the two losses to tradeoff source risk and domain discrepancy.

The training procedures of CLARINET are shown in Algorithm 2. First, we initialize the whole network (line 1) and shuffle the training set (line 3). During each epoch, after mini-batch $\overline{d}_s$ and d_t are fetched (line 5), we divide the source mini-batch $\overline{d}_s$ into $\{\overline{d}_{s,k}\}_{k=1}^K$ using Eq. (19) (line 6). Then, $\{\overline{d}_{s,k}\}_{k=1}^K$ are used to calculate the complementary-label loss for each class (i.e., $\{\overline{L}_s(G, F, \overline{d}_{s,k})\}_{k=1}^K$) and the whole complementary-label loss $\overline{L}_s(G, F, \overline{d}_s)$ (line 7).

If $\min_k\{\overline{L}_s(G, F, \overline{d}_{s,k})\}_{k=1}^K \geq 0$, we calculate the gradient $\nabla \overline{L}_s(G, F, \overline{d}_s)$ and update parameters of G and F using gradient descent (lines 8-9). Otherwise, we sum negative elements in $\{\overline{L}_s(G, F, \overline{d}_{s,k})\}_{k=1}^K$ as $\overline{L}_{neg}$ (line 11) and calculate the gradient with $\nabla \overline{L}_{neg}$ (line 12). Then, we update parameters of G and F using gradient ascent (line 12), which is suggested by [41]. When the number of epochs (i.e., t) is over T_s, we start to update parameters of D (line 14). We calculate the scattered conditional adversarial loss L_{adv} (line 15). Then, L_{adv} is minimized over D (line 16), but maximized over $F\circ G$ (line 17) for adversarial training.

In this paragraph, we analyze the time complexity of training CLARINET. Let $C1$ denote the cost of computing (21), and $C2$ denote the cost of computing (24). The each epoch of training in Algorithm 2 costs $\mathcal{O}\ (mC1 + mC2)$, where m is the number of batches in each epoch.

C. CLARINET for PC-UDA Tasks

For PC-UDA tasks, we have both complementary-label data and true-label data in the source domain. In such cases, we want to leverage both kinds of labeled source data to help realize better adaptation results. The two loss functions mentioned in Section V-A are adjusted as follows.

After obtaining mini-batch d_s from D_s, we could calculate the classification loss based on true-label data by

$$L_s(G, F, d_s) = \ell(F \circ G(\mathbf{x}_i), \mathbf{y}_i), \tag{26}$$

where ℓ is cross-entropy loss, $d_s = \{(\mathbf{x}_i, y_i)\}_{i=1}^{n_s'}$ and $n_s' = |d_s|$. We could use a convex combination of classification risks derived from true-label data and complementary-label data to replace the oral complementary-label based only classification risk shown as follows.

$$L_c = \alpha L_s(G, F, d_s) + (1-\alpha)\overline{L}_s(G, F, \overline{d}_s), \tag{27}$$

where α depends on the cost of labeling the two kind of data.

The new scattered conditional adversarial loss for PC-UDA tasks is as follows.

$$\begin{aligned} & L_{adv}(G, F, D, d_s, \overline{d}_s, d_t) \\ = & -\frac{\sum_{\mathbf{x}\in d_s[X]} \omega_s(\mathbf{x}) \log(D(\boldsymbol{g}(\mathbf{x})))}{\sum_{\mathbf{x}\in d_s[X]} \omega_s(\mathbf{x})} \\ & -\frac{\sum_{\mathbf{x}\in \overline{d}_s[X]} \omega_{\overline{s}}(\mathbf{x}) \log(D(\boldsymbol{g}(\mathbf{x})))}{\sum_{\mathbf{x}\in \overline{d}_s[X]} \omega_{\overline{s}}(\mathbf{x})} \\ & -\frac{\sum_{\mathbf{x}\in d_t} \omega_t(\mathbf{x}) \log(1 - D(\boldsymbol{g}(\mathbf{x})))}{\sum_{\mathbf{x}\in d_t} \omega_t(\mathbf{x})}, \end{aligned} \tag{28}$$

where $\omega_s(\mathbf{x})$, $\omega_{\overline{s}}(\mathbf{x})$ and $\omega_t(\mathbf{x})$ are $1 + e^{-H(G,F,\mathbf{x})}$, $\boldsymbol{g}(\mathbf{x})$ is $G(\mathbf{x}) \otimes T(F \circ G(\mathbf{x}))$, $d_s[X]$ and $\overline{d}_s[X]$ is the feature part of d_s and $\overline{d}_s$. The entire training procedures of CLARINET for PC-UDA are shown in Algorithm 3.

VI. Experiments

This section conducts extensive evaluations of CLARINET on several common transfer tasks against many state-of-the-art transfer learning methods (e.g., two-step approach).

A. Datasets and Tasks

We investigate seven image and digits datasets: *CIFAR-10* [69], *STL* [70], *MNIST* [71], *USPS* [72], *SVHN* [73], *MNIST-M* [74] and *SYN-DIGITS* [74]. We adopt the evaluation protocol of DANN [19], CDAN [20], ATDA [12], and DIRT-T [75] with seven transfer tasks: *CIFAR-10* to *STL* (*C* $\rightarrow$ *T*), *MNIST* to *USPS* (*M* $\rightarrow$ *U*), *USPS* to *MNIST* (*U* $\rightarrow$ *M*), *SVHN* to *MNIST* (*S* $\rightarrow$ *M*), *MNIST* to *MNIST-M* (*M* $\rightarrow$ *m*), *SYN-DIGITS* to *MNIST* (*Y* $\rightarrow$ *M*) and *SYN-DIGITS* to *SVHN* (*Y* $\rightarrow$ *S*).

We train our model using the training sets: *CIFAR-10* $(45,000)$, *STL* $(4,500)$, *MNIST* $(60,000)$, *USPS* $(7,438)$, *SVHN* $(73,257)$, *MNIST-M* $(59,001)$, *SYN-DIGITS* $(479,400)$. Evaluation is reported on the standard test sets: *STL* $(7,200)$, *MNIST* $(10,000)$, *USPS* $(1,860)$, *MNIST-M* $(9,001)$, *SVHN* $(26,032)$ (the numbers of images are in parentheses).

Since all datasets carry true labels, following [41], we generate completely and partly complementary-label data. Generating complementary-label data is straightforward when the dataset is ordinary-labeled, as it reduces to just choosing a class randomly other than true class.

B. Baselines

We compare CLARINET with the following baselines: *gradient ascent complementary label learning* (GAC) [41], namely non-transfer method, and several two-step methods, which sequentially combine GAC with UDA methods (including DAN [17], DANN [19] and CDAN [20]). Thus, we have four possible baselines: GAC, GAC+DAN, GAC+DANN and GAC+CDAN. For two-step methods, they share the same pseudo-label source data on each task. Note that, in this paper, we use the entropy conditioning variant of CDAN (CDAN_E).

C. Experimental Setup

We follow the standard protocols for unsupervised domain adaptation and compare the average classification accuracy based on 5 random experiments. For each experiment, we take the result of the last epoch.

The batch size is set to 128 and we train 500 epochs. SGD optimizer (momentum= 0.9, weight_decay= $5e-5$) is with an initial learning rate of 0.005 in the adversarial network and $5e-5$ in the classifier. In the sharpening function T, l is set to 0.5. For other special parameters in baselines, we all follow the original setting. We implement all methods with default parameters by PyTorch. The code of CLARINET is available at github.com/Yiyang98/BFUDA.

D. Results on CC-UDA Tasks

Table I reports the target-domain accuracy of 5 methods on 7 CC-UDA tasks. As can be seen, our CLARINET performs best on each task and the average accuracy of CLARINET is significantly higher than those of baselines. Compared with GAC method, CLARINET successfully transfers knowledge from complementary-label source data to unlabeled target data. Since CDAN has shown much better adaptation performance than DANN and DAN [20], GAC+CDAN should outperform other two-step methods on each task. However, on the $U \rightarrow M$ task, the accuracy of GAC+CDAN is much lower than that of GAC+DANN. This abnormal phenomenon shows that the noise contained in pseudo-label source data significantly reduces transferability of existing UDA methods. Namely, we cannot obtain the reliable adaptation performance by using two-step CC-UDA approach.

***CIFAR-10* $\rightarrow$ *STL*.** CIFAR-10 and STL are 10-class object recognition datasets. We remove the non-overlapping classes ("frog" and "monkey") and readjust the labels to align the two datasets. Namely this task is reduced to a 9-class classification problem. Furthermore, we downscale the 96×96 image dimension of STL to match the 32×32 dimension of CIFAR-10. As shown in Figure 4 (a), two-step methods could hardly transfer knowledge, while our CLARINET's performance surpasses others by a comfortable margin.

***MNIST* $\leftrightarrow$ *USPS*.** MNIST and USPS are both grayscale digits images, thus the distribution discrepancy between the two tasks is relatively small. As shown in Figure 4 (b) and (c), in both adaptation directions, CLARINET all achieve the best performance far above other baselines.

***SVHN* $\rightarrow$ *MNIST*.** SVHN and MNIST are both digit datasets. Whereas MNIST consists of black-and-white handwritten digits, SVHN consists of crops of colored, street house numbers. MNIST has a lower image dimensionality than SVHN, thus we adopt the dimension of MNIST to 32×32 with three channels to match SVHN. Because of the above factors, the gap between two distributions are relatively larger compared to that of the *MNIST* $\leftrightarrow$ *USPS*. As shown in Figure 4 (d), GAC+CDAN performs much better than GAC+DAN and GAC+DANN, but still worse than our CLARINET.

***MNIST* $\rightarrow$ *MNIST-M*.** MNIST-M is a transformed dataset from MNIST, which is composed by merging clips of a background from the BSDS500 datasets [76]. For a human, the classification task on MNIST-M only becomes slightly harder, whereas for a CNN network trained on MNIST, this domain is quite different, as the background and the strokes are no longer constant. As shown in Figure 4 (e), Our method is slightly more effective than GAC+CDAN and far more effective than the other two methods.

***SYN-DIGITS* $\rightarrow$ *MNIST*.** This adaptation reflects a common adaptation problem of transferring from synthetic images to real images. The SYN-DIGITS dataset consists of a huge amount of data, generated from Windows fonts by varying the text, positioning, orientation, background, stroke color, and the amount of blur. As shown in Figure 4 (f), our method outperforms other baselines and achieves pretty high accuracy. Thus with sufficient source data, CLARINET could achieve excellent results.

***SYN-DIGITS* $\rightarrow$ *SVHN*.** This adaptation is another common adaptation problem of transferring from synthetic images to real images, but is more challenging than in the case of the MNIST experiment. As shown in Figure 4 (g), our method is

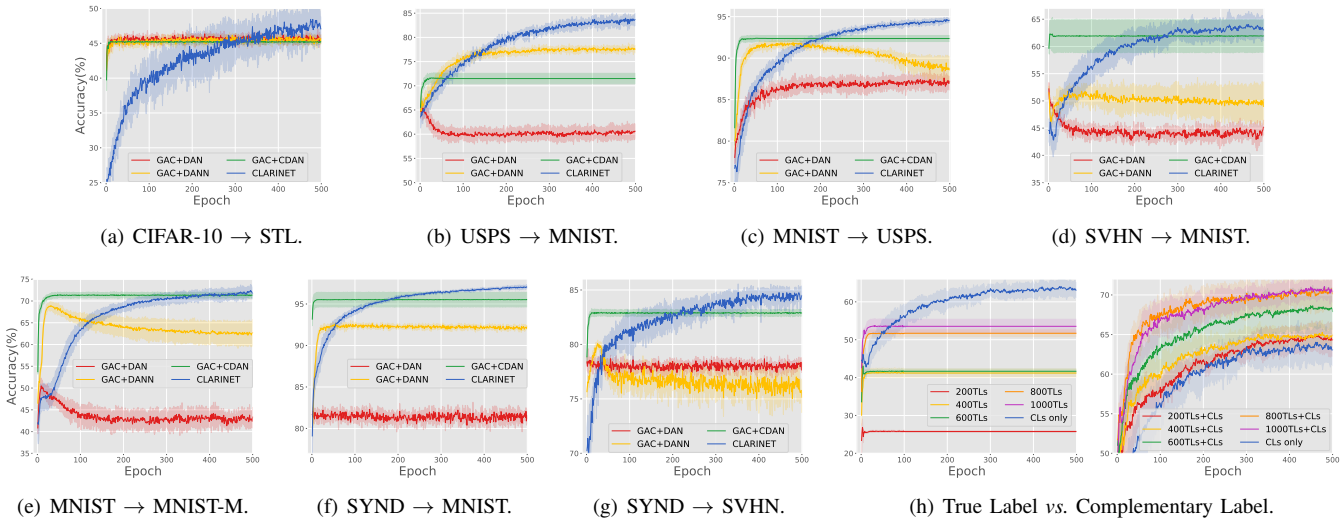

(a) CIFAR-10 → STL. (b) USPS → MNIST. (c) MNIST → USPS. (d) SVHN → MNIST.

(e) MNIST → MNIST-M. (f) SYND → MNIST. (g) SYND → SVHN. (h) True Label *vs.* Complementary Label.

Fig. 4: Test Accuracy vs. Epochs on 7 CC-UDA Tasks in (a)-(g), and *True Label* (TL) vs. *Complementary Label* (CL) in (h). In (a)-(g), we compare the target-domain accuracy of one-step approach, i.e., CLARINET (*ours*), with that of two-step approach (*ours*). In (h), "200TLs" represents ordinary UDA method trained with 200 true-label source data. "200TLs+CLs" means a CLARINET trained with 200 true-label source data and complementary-label source data and "CLs Only" represents a CLARINET trained with complementary-label source data.

TABLE I: Results on 7 CC-UDA Tasks. Bold value represents the highest accuracy (%) on each row. Please note, the two-step methods and CLARINET are all first proposed in our paper.

Tasks	GAC	Two-step approaches (*ours*)			CLARINET (*ours*)
		GAC+DAN	GAC+DANN	GAC+CDAN_E	
$C \rightarrow T$	45.167	45.711±0.535	45.628±0.572	45.228±0.270	**47.083±1.395**
$U \rightarrow M$	51.860	60.692±1.300	77.580±0.770	71.498±1.077	**83.692±0.928**
$M \rightarrow U$	77.796	87.215±0.603	88.688±1.280	92.366±0.365	**94.538±0.292**
$S \rightarrow M$	39.260	45.132±1.363	50.882±2.440	61.922±2.983	**63.070±1.990**
$M \rightarrow m$	45.045	43.346±2.224	62.273±2.261	71.379±0.620	**71.717±1.262**
$Y \rightarrow M$	77.070	81.150±0.591	92.328±0.138	95.532±0.873	**97.040±0.212**
$Y \rightarrow S$	72.480	78.270±0.311	75.147±1.401	82.878±0.278	**84.499±0.537**
Average	58.383	63.074	70.361	74.400	**77.377**

obviously more effective than other baselines. GAC+DANN does not apply to this task, achieving the lowest accuracy.

E. Results on PC-UDA Tasks

Table II reports the target-domain accuracy of CLARINET on PC-UDA tasks with different amounts of true-label source data. "true only" means training on a certain number of true-label source data with ordinary UDA method. "com only" means training on complementary-label source data only with CLARINET. "com+true" stands for training on a certain number of true-label source data and complementary-label source data with CLARINET. In general, the accuracy of CLARINET increases when increasing the amount of true-label source data from 0 to 1000. Thus, it is proved that CLARINET can sufficiently leverage true-label source data to improve adaptation performance.

The improvement is especially evident on $U \rightarrow M$ task and $S \rightarrow M$ task. For $U \rightarrow M$ task, this is probably because the dataset sample size of USPS is relatively small, true-label data actually has occupied a big part. For $S \rightarrow M$ task, SVHN is complicated for complementary-label learning. Hence adding a small amount of true-label data could help to train a more accurate classifier. This phenomenon also reminds us that for complex datasets, adding some true-label data to assist training would be pretty appropriate. On $Y \rightarrow M$ task, adding true-label source data does not bring significant improvement, which is most likely due to the result on complementary-label data is already relatively good and true-label source data is unable to assist in achieving better result.

We also compare the efficacy of true-label source data with complementary-label source data. Taking $S \rightarrow M$ task as an example (as shown in the left part of Figure 4 (h)), we compare the target-domain accuracy of ordinary UDA method trained with different amount of true-label source data and that of CLARINET trained with complementary-label source data only ("CLs Only"). The accuracy decreases significantly when reducing the amount of true-label source data, which suggests that sufficient true-label source data are inevitably required in UDA scenario. Then we compare the target-domain accuracy of CLARINET trained with complementary-label source data only with that of CLARINET trained with different amount of true-label and complementary-label source data. It is clear that CLARINET effectively uses two kinds of data to obtain better adaptation performance than using complementary-label

TABLE II: Results on 7 PC-UDA Tasks. Amount represents the number of true-label data in the source domain. In general, the accuracy of CLARINET increases when increasing the amount of true-label source data.

Tasks	Amount of of true-label source data					
	0		200		400	
	true only	com only	true only	com+true	true only	com+true
$C \to T$	-	47.083±1.395	11.839±0.019	49.408±1.776	13.875±1.366	49.553±1.362
$U \to M$	-	83.692±0.928	74.180±1.218	88.584±1.040	79.200±0.837	89.480±1.660
$M \to U$	-	94.538±0.292	78.011±1.473	93.204±1.398	83.204±1.545	94.677±0.576
$S \to M$	-	63.070±1.990	25.772±0.146	64.734±2.096	41.232±1.089	64.912±0.928
$M \to m$	-	71.717±1.262	59.414±1.381	70.730±1.620	59.805±0.951	71.198±0.623
$Y \to M$	-	97.040±0.212	49.232±1.354	97.182±0.383	60.640±1.570	97.242±0.117
$Y \to S$	-	84.499±0.537	23.009±1.102	84.269±0.814	49.120±1.236	85.538±0.596
Average	-	77.377	45.922	78.302	55.297	78.943
Tasks	600		800		1000	
	true only	com+true	true only	com+true	true only	com+true
$C \to T$	17.722±2.626	50.897±0.969	19.278±0.853	51.058±1.737	20.972±1.061	53.297±1.655
$U \to M$	82.532±0.859	90.358±1.938	85.800±0.621	91.106±0.561	88.184±1.280	93.342±1.294
$M \to U$	83.925±1.511	94.839±0.254	85.839±2.074	94.796±0.104	85.699±0.777	95.022±0.280
$S \to M$	41.680±0.525	67.898±1.625	51.652±0.850	70.416±1.819	53.500±1.872	70.446±1.358
$M \to m$	63.757±1.344	72.732±0.947	65.161±0.766	73.050±1.264	68.522±1.285	73.336±0.727
$Y \to M$	76.802±1.649	97.178±0.396	85.286±1.363	96.842±0.267	86.470±1.646	96.948±0.266
$Y \to S$	67.922±1.079	85.921±1.098	67.788±1.878	86.772±0.291	74.654±1.054	87.024±0.542
Average	62.049	79.975	65.829	80.577	68.286	81.345

TABLE III: Ablation Study. Bold value represents the highest accuracy (%) on each column. Obviously to see, UDA methods cannot handle complementary-label based UDA tasks directly. We also prove that the conditioning adversarial part and the sharpening function T can help improve the adaptation performance.

Methods	$C \to T$	$U \to M$	$M \to U$	$S \to M$	$M \to m$	$Y \to M$	$Y \to S$	Average
C w/ L_{CE}	6.481±2.536	0.455±0.722	0.055±0.129	3.708±0.688	7.088±0.424	1.832±0.102	1.298±0.070	2.987
C w/o c	41.908±2.796	**84.302±1.127**	93.301±0.465	44.500±2.088	70.994±0.749	94.382±0.150	83.408±0.545	73.256
C w/o T	43.075±2.553	83.192±1.796	93.419±0.588	52.438±1.927	**72.128±1.569**	95.442±1.004	83.055±0.652	74.678
CLARINET	**47.083±1.395**	83.692±0.928	**94.538±0.292**	**63.070±1.990**	71.717±1.262	**97.040±0.212**	**84.499±0.537**	**77.377**

source data only. Besides, as the number of true-label source data used increases, the classification accuracy becomes higher (as shown in the right part of Figure 4 (h)).

F. Analysis

1) Labeling Cost: From a theoretical analysis, the information carried by the true label is $K-1$ times that of the complementary label. We conduct experiments and prove the ratio is actually far less than $K-1$ when obtaining the same result, which means using complementary label is low-cost. More detailed analysis can be found in Appendix C.

2) Ablation Study: We conduct experiments to show the contributions of different components in CLARINET. We consider following baselines:

- C w/ L_{CE}: train CLARINET by Algorithm 2, while replacing $\overline{L}_s(G, F, \overline{D}_s)$ by cross-entropy loss.
- C w/o c : train CLARINET without conditioning, namely train the domain discriminator D only based on feature representations g_s and g_t.
- C w/o T: train CLARINET by Algorithm 2, without sharpening function T.

C w/ L_{CE} uses the cross-entropy loss to take place of complementary-label loss. Actually, it stands for applying ordinary UDA methods directly on complementary-label based UDA tasks. The target-domain accuracy of C w/ L_{CE} will show whether UDA methods can address the complementary-label based UDA problem. C w/o c train the domain discriminator D only based on feature representations g_s and g_t, thus the result could indicate whether the conditional adversarial way could capture the multimodal structures so as to improve the transfer effect. Please notice, the sharpening function T is useless in this network as it works on the label prediction f_s and f_t. Comparing CLARINET with C w/o T reveals if the sharpening function T takes effect.

As shown in Table III, the target-domain accuracy of C w/ L_{CE} is much lower than that of other methods. Namely, UDA methods cannot handle complementary-label based UDA tasks directly. Its result is not even as good as random classification, as the network is trained taking the wrong label as the target result. Compared with C w/o T, C w/o c has a worse performance, which proves that the conditional adversarial way could really improve the transfer effect. Therefore, it is necessary to capture the multimodal structures of distributions with cross-covariance dependency between the features and classes in the field of adversarial based UDA. Although C w/o T achieves better accuracy than other baselines, its accuracy still worse than CLARINET's. The result reveals that the sharpening function T helps to capture multimodal

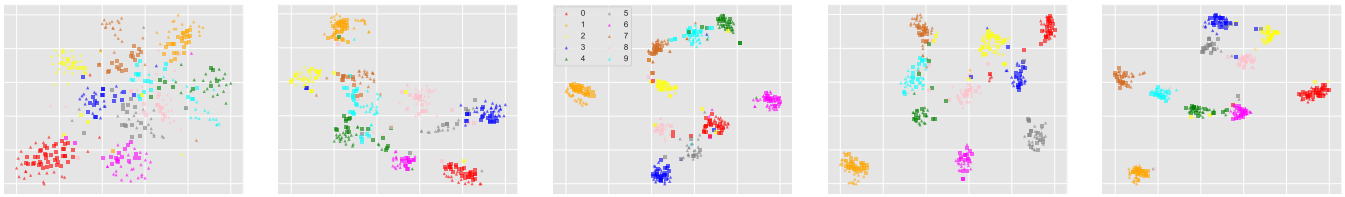

(a) GAC. (b) GAC+DAN. (c) GAC+DANN. (d) GAC+CDAN. (e) CLARINET.

Fig. 5: Feature visualization of target and source features on $M \rightarrow U$ task. $\triangle$ indicates source samples. $\square$ indicates target samples. Different colors indicate different classes.

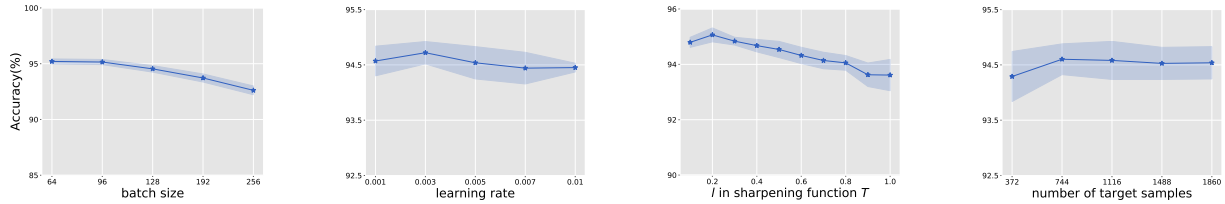

(a) (b) (c) (d)

Fig. 6: Parameter analyses. Hyper-parameter sensitivity studies are carried out to find their effect on the performance. Experiments are conducted on $M \rightarrow U$ task. In (a)-(d), we show how these 4 parameters influence the test accuracy.

structures of distributions on basis of the characteristics of complementary-label learning. Thus, the sharpening function T can improve the adaptation performance.

3) Visualization: In order to intuitively demonstrate the effect of our method, we show the feature visualization of source and target domains by t-SNE [77], which is an effective dimensionality reduction method. Figure 5 shows the effect of domain adaptation of all the baselines and our method in $M \rightarrow U$ task. Clearly, our method outperforms baselines in aligning the distributions of two domains.

In Figure 5 (a), although the samples of two domains tend to gather in general, they are not actually tightly clustered together, and the class 9 (cyan) is an obvious example. As GAC is a non-transfer method, it could be used to compare the effect of before-after domain discrepancy with other methods. In Figure 5 (e), it is cleraly that the intra-class centroids of two domains are closer than other baselines and there are fewer error clustered samples, namely CLARINET does better in aligning the distributions of source and target domains.

4) Parameter Analysis: To investigate their effect on the performance, we carry out hyper-parameter sensitivity studies. Taking $M \rightarrow U$ task for example, we conduct experiments to demonstrate the effect of 4 parameters for our method, including batch size, learning rate, l in sharpening function T and the number of unlabeled target domain samples.

As shown in Figure 6, the accuracy of CLARINET decreases in general when increasing the batch size from 64 to 256. We increase the learning rate from 0.001 to 0.01, and it achieves the best result at 0.003. The l in sharpening function T is an important parameter for CLARINET, as the sharpening function T could effectively help improve the adaptation performance. It could be seen that when l is small, namely the output of sharpening function T approaches an one-hot distribution, CLARINET could achieve a good result in this task. We also test how the number of target samples would affect the performance. As shown in Figure 6 (d), when sufficient samples are available, the accuracy stays stable.

VII. Conclusion and Further Study

This paper presents a new setting, complementary-label based UDA, which exploits economical complementary-label source data instead of expensive true-label source data. We consider two cases of the complementary-label based UDA: one is that the source domain only contains complementary-label data (CC-UDA), and the other is that the source domain has plenty of complementary-label data and a small amount of true-label data (PC-UDA). Since existing UDA methods cannot address the complementary-label based UDA problem, we propose a novel one-step approach called *complementary label adversarial network* (CLARINET). CLARINET can handle both CC-UDA and PC-UDA tasks. Experiments conducted on 7 complementary-label based UDA tasks confirm that CLARINET effectively achieves distributional adaptation from complementary-label source data to unlabeled target data and outperforms a series of competitive baselines.

In the future, we plan to explore more effective ways to solve complementary-label based UDA and extend the application of complementary labels in domain adaptation. For example, instead of requiring the source domain and the target domain to share the same label set, we could apply complementary labels in the open set domain adaptation scenario in which the target domain contains unknown classes that are not observed in the source domain.

Acknowledgements

The work presented in this paper was supported by the Australian Research Council (ARC) under FL190100149. The first author particularly thanks the support by UTS-AAII during her visit.

REFERENCES

[1] Y. Luo, Y. Wen, T. Liu, and D. Tao, "Transferring knowledge fragments for learning distance metric from a heterogeneous domain," *TPAMI*, pp. 1013–1026, 2019.

[2] M. Xiao and Y. Guo, "Feature space independent semi-supervised domain adaptation via kernel matching," *TPAMI*, pp. 54–66, 2014.

[3] K. Zhang, B. Schölkopf, K. Muandet, and Z. Wang, "Domain adaptation under target and conditional shift," in *ICML*, 2013, pp. 819–827.

[4] L. Zhong, Z. Fang, F. Liu, J. Lu, B. Yuan, and G. Zhang, "How does the combined risk affect the performance of unsupervised domain adaptation approaches?" in *AAAI*, 2021.

[5] S. Motiian, M. Piccirilli, D. Adjeroh, and G. Doretto, "Unified deep supervised domain adaptation and generalization," in *ICCV*, 2017, pp. 5715–5725.

[6] S. Sukhija, N. Krishnan, and G. Singh, "Supervised heterogeneous domain adaptation via random forests." in *IJCAI*, 2016, pp. 2039–2045.

[7] E. Tzeng, J. Hoffman, T. Darrell, and K. Saenko, "Simultaneous deep transfer across domains and tasks," in *ICCV*, 2015, pp. 4068–4076.

[8] L. Cheng and S. J. Pan, "Semi-supervised domain adaptation on manifolds," *TNNLS*, pp. 2240–2249, 2014.

[9] S. Mehrkanoon and J. A. K. Suykens, "Regularized semipaired kernel CCA for domain adaptation," *TNNLS*, pp. 3199–3213, 2018.

[10] K. Islam, V. Hill, B. Schaeffer, R. Zimmerman, and J. Li, "Semi-supervised adversarial domain adaptation for seagrass detection in multispectral images," in *ICDM*, 2019, pp. 1120–1125.

[11] P. Wei, Y. Ke, and C. K. Goh, "Feature analysis of marginalized stacked denoising autoenconder for unsupervised domain adaptation," *TNNLS*, pp. 1321–1334, 2019.

[12] K. Saito, Y. Ushiku, and T. Harada, "Asymmetric tri-training for unsupervised domain adaptation," in *ICML*, 2017, pp. 2988–2997.

[13] Y. Cao, M. Long, and J. Wang, "Unsupervised domain adaptation with distribution matching machines," in *AAAI*, 2018, pp. 2795–2802.

[14] Z. Deng, Y. Luo, and J. Zhu, "Cluster alignment with a teacher for unsupervised domain adaptation," in *ICCV*, 2019, pp. 9944–9953.

[15] S. Zhao, H. Fu, M. Gong, and D. Tao, "Geometry-aware symmetric domain adaptation for monocular depth estimation," in *CVPR*, 2019, pp. 9788–9798.

[16] G. Agresti, H. Schäfer, P. Sartor, and P. Zanuttigh, "Unsupervised domain adaptation for tof data denoising with adversarial learning," in *CVPR*, 2019, pp. 5584–5593.

[17] M. Long, Y. Cao, J. Wang, and M. I. Jordan, "Learning transferable features with deep adaptation networks," in *ICML*, 2015, pp. 97–105.

[18] M. Long, H. Zhu, J. Wang, and M. I. Jordan, "Deep transfer learning with joint adaptation networks," in *ICML*, 2017, pp. 2208–2217.

[19] Y. Ganin, E. Ustinova, H. Ajakan, P. Germain, H. Larochelle, F. Laviolette, M. Marchand, and V. Lempitsky, "Domain-adversarial training of neural networks," *JMLR*, pp. 1–35, 2016.

[20] M. Long, Z. Cao, J. Wang, and M. Jordan, "Conditional adversarial domain adaptation," in *NeurIPS*, 2018, pp. 1640–1650.

[21] M. Gong, K. Zhang, T. Liu, D. Tao, C. Glymour, and B. Schölkopf, "Domain adaptation with conditional transferable components," in *ICML*, 2016, pp. 2839–2848.

[22] K. Zhang, M. Gong, and B. Schölkopf, "Multi-source domain adaptation: A causal view," in *AAAI*, 2015, pp. 3150–3157.

[23] S. Sankaranarayanan, Y. Balaji, C. Castillo, and R. Chellappa, "Generate to adapt: Aligning domains using generative adversarial networks," in *CVPR*, 2018, pp. 8503–8512.

[24] T. Ishida, G. Niu, W. Hu, and M. Sugiyama, "Learning from complementary labels," in *NeurIPS*, 2017, pp. 5639–5649.

[25] X. Yu, T. Liu, M. Gong, and D. Tao, "Learning with biased complementary labels," in *ECCV*, 2018, pp. 69–85.

[26] F. Liu, J. Lu, B. Han, G. Niu, G. Zhang, and M. Sugiyama, "Butterfly: A panacea for all difficulties in wildly unsupervised domain adaptation," in *NeurIPS LTS Workshop*, 2019.

[27] Y. Shu, Z. Cao, M. Long, and J. Wang, "Transferable curriculum for weakly-supervised domain adaptation," in *AAAI*, 2019, pp. 4951–4958.

[28] Y. Zhang, L. Feng, Z. Fang, B. Yuan, G. Zhang, and J. Lu, "Clarinet: A one-step approach towards budget-friendly unsupervised domain adaptation," in *IJCAI*, 2020.

[29] L. Song, J. Huang, A. Smola, and K. Fukumizu, "Hilbert space embeddings of conditional distributions with applications to dynamical systems," in *ICML*, 2009, pp. 961–968.

[30] R. Gopalan, R. Li, and R. Chellappa, "Domain adaptation for object recognition: An unsupervised approach," in *ICCV*, 2011, pp. 999–1006.

[31] B. Gong, Y. Shi, F. Sha, and K. Grauman, "Geodesic flow kernel for unsupervised domain adaptation," in *CVPR*, 2012, pp. 2066–2073.

[32] J. Hoffman, S. Guadarrama, E. Tzeng, R. Hu, J. Donahue, R. Girshick, T. Darrell, and K. Saenko, "Lsda: Large scale detection through adaptation," in *NeurIPS*, 2014, pp. 3536–3544.

[33] R. Collobert, J. Weston, L. Bottou, M. Karlen, K. Kavukcuoglu, and P. Kuksa, "Natural language processing (almost) from scratch," *JMLR*, pp. 2493–2537, 2011.

[34] X. Glorot, A. Bordes, and Y. Bengio, "Domain adaptation for large-scale sentiment classification: A deep learning approach," in *ICML*, 2011, pp. 513–520.

[35] J. Huang, A. Gretton, K. Borgwardt, B. Schölkopf, and A. J. Smola, "Correcting sample selection bias by unlabeled data," in *NeurIPS*, 2007, pp. 601–608.

[36] S. J. Pan, I. W. Tsang, J. T. Kwok, and Q. Yang, "Domain adaptation via transfer component analysis," *TNNLS*, pp. 199–210, 2010.

[37] Y. Bengio, A. Courville, and P. Vincent, "Representation learning: A review and new perspectives," *TPAMI*, pp. 1798–1828, 2013.

[38] J. Yosinski, J. Clune, Y. Bengio, and H. Lipson, "How transferable are features in deep neural networks?" in *NeurIPS*, 2014, pp. 3320–3328.

[39] F. Liu, W. Xu, J. Lu, G. Zhang, A. Gretton, and D. J. Sutherland, "Learning deep kernels for non-parametric two-sample tests," in *ICML*, 2020.

[40] K. Bousmalis, N. Silberman, D. Dohan, D. Erhan, and D. Krishnan, "Unsupervised pixel-level domain adaptation with generative adversarial networks," in *CVPR*, 2017, pp. 3722–3731.

[41] T. Ishida, G. Niu, A. Menon, and M. Sugiyama, "Complementary-label learning for arbitrary losses and models," in *ICML*, 2019, pp. 2971–2980.

[42] K. Lee, X. He, L. Zhang, and L. Yang, "Cleannet: Transfer learning for scalable image classifier training with label noise," in *CVPR*, 2018, pp. 5447–5456.

[43] F. Schroff, A. Criminisi, and A. Zisserman, "Harvesting image databases from the web," *TPAMI*, pp. 754–766, 2011.

[44] Y. Zhang, T. Liu, M. Long, and M. Jordan, "Bridging theory and algorithm for domain adaptation," in *ICML*, 2019, pp. 7404–7413.

[45] Z. Fang, J. Lu, F. Liu, J. Xuan, and G. Zhang, "Open set domain adaptation: Theoretical bound and algorithm," *TNNLS*, 2020.

[46] M. Ghifary, D. Balduzzi, W. B. Kleijn, and M. Zhang, "Scatter component analysis: A unified framework for domain adaptation and domain generalization," *TPAMI*, pp. 1414–1430, 2017.

[47] A. Kumar, P. Sattigeri, and T. Fletcher, "Semi-supervised learning with gans: Manifold invariance with improved inference," in *NeurIPS*, 2017, pp. 5534–5544.

[48] B. Frénay and M. Verleysen, "Classification in the presence of label noise: A survey," *TNNLS*, pp. 845–869, 2014.

[49] Y. Li and Z. Zhou, "Towards making unlabeled data never hurt," *TPAMI*, pp. 175–188, 2015.

[50] T. Sakai, M. du Plessis, G. Niu, and M. Sugiyama, "Semi-supervised classification based on classification from positive and unlabeled data," in *ICML*, 2017, pp. 2998–3006.

[51] B. Han, Q. Yao, X. Yu, G. Niu, M. Xu, W. Hu, I. Tsang, and M. Sugiyama, "Co-teaching: Robust training of deep neural networks with extremely noisy labels," in *NeurIPS*, 2018, pp. 8527–8537.

[52] B. Han, J. Yao, G. Niu, M. Zhou, I. Tsang, Y. Zhang, and M. Sugiyama, "Masking: A new perspective of noisy supervision," in *NeurIPS*, 2018, pp. 5836–5846.

[53] Q. Miao, Y. Cao, G. Xia, M. Gong, J. Liu, and J. Song, "Rboost: Label noise-robust boosting algorithm based on a nonconvex loss function and the numerically stable base learners," *TNNLS*, pp. 2216–2228, 2016.

[54] E. Xing, M. Jordan, S. Russell, and A. Ng, "Distance metric learning with application to clustering with side-information," in *NeurIPS*, 2003, pp. 521–528.

[55] T. F. Covoes, E. R. Hruschka, and J. Ghosh, "Competitive learning with pairwise constraints," *TNNLS*, pp. 164–169, 2013.

[56] J. Goldberger, G. Hinton, S. Roweis, and R. Salakhutdinov, "Neighbourhood components analysis," in *NeurIPS*, 2005, pp. 513–520.

[57] M. Du Plessis, G. Niu, and M. Sugiyama, "Analysis of learning from positive and unlabeled data," in *NeurIPS*, 2014, pp. 703–711.

[58] G. Niu, M. du Plessis, T. Sakai, Y. Ma, and M. Sugiyama, "Theoretical comparisons of positive-unlabeled learning against positive-negative learning," in *NeurIPS*, 2016, pp. 1199–1207.

[59] C. Gong, T. Liu, J. Yang, and D. Tao, "Large-margin label-calibrated support vector machines for positive and unlabeled learning," *TNNLS*, pp. 3471–3483, 2019.

[60] R. Kiryo, G. Niu, M. du Plessis, and M. Sugiyama, "Positive-unlabeled learning with non-negative risk estimator," in *NeurIPS*, 2017, pp. 1675–1685.

[61] G. Agresti, H. Schaefer, P. Sartor, and P. Zanuttigh, "Unsupervised domain adaptation for tof data denoising with adversarial learning," in *CVPR*, 2019, pp. 5584–5593.

[62] I. Goodfellow, J. Pouget-Abadie, M. Mirza, B. Xu, D. Warde-Farley, S. Ozair, A. Courville, and Y. Bengio, "Generative adversarial nets," in *NeurIPS*, 2014, pp. 2672–2680.

[63] S. Arora, R. Ge, Y. Liang, T. Ma, and Y. Zhang, "Generalization and equilibrium in generative adversarial nets (gans)," in *ICML*, 2017, pp. 224–232.

[64] M. Mirza and S. Osindero, "Conditional generative adversarial nets," *CoRR*, 2014.

[65] A. Odena, C. Olah, and J. Shlens, "Conditional image synthesis with auxiliary classifier gans," in *ICML*, 2017, pp. 2642–2651.

[66] I. Goodfellow, Y. Bengio, and A. Courville, *Deep learning*. MIT press, 2016.

[67] D. Berthelot, N. Carlini, I. Goodfellow, N. Papernot, A. Oliver, and C. A. Raffel, "Mixmatch: A holistic approach to semi-supervised learning," in *NeurIPS*, 2019, pp. 5050–5060.

[68] X. Zhu, Z. Ghahramani, and J. Lafferty, "Semi-supervised learning using gaussian fields and harmonic functions," in *ICML*, 2003, pp. 912–919.

[69] A. Krizhevsky, G. Hinton *et al.*, "Learning multiple layers of features from tiny images," *Master's thesis*, 2009.

[70] A. Coates, A. Ng, and H. Lee, "An analysis of single-layer networks in unsupervised feature learning," in *AISTATS*, 2011, pp. 215–223.

[71] Y. LeCun, L. Bottou, Y. Bengio, and P. Haffner, "Gradient-based learning applied to document recognition," *Proceedings of the IEEE*, pp. 2278–2324, 1998.

[72] T. Hastie, J. Friedman, and R. Tibshirani, *The Elements of Statistical Learning: Data Mining, Inference, and Prediction*, 2001.

[73] Y. Netzer, T. Wang, A. Coates, A. Bissacco, B. Wu, and A. Ng, "Reading digits in natural images with unsupervised feature learning," in *NeurIPS DLUFL Workshop*, 2011.

[74] Y. Ganin and V. Lempitsky, "Unsupervised domain adaptation by backpropagation," in *ICML*, 2015, pp. 1180–1189.

[75] R. Shu, H. Bui, H. Narui, and S. Ermon, "A DIRT-T approach to unsupervised domain adaptation," in *ICLR*, 2018.

[76] P. Arbelaez, M. Maire, C. Fowlkes, and J. Malik, "Contour detection and hierarchical image segmentation," *TPAMI*, pp. 898–916, 2010.

[77] L. v. d. Maaten and G. Hinton, "Visualizing data using t-sne," *JMLR*, 2008.

Yiyang Zhang received her B.E. degree in Automation from Tsinghua University, P.R. China, in 2018. She is currently a Master student in Data Science at Shenzhen International Graduate School, Tsinghua University, and a visiting student with the Australian Artificial Intelligence Institute (AAII), the University of Technology, Sydney (UTS). Her research interests include transfer learning and domain adaptation.

Feng Liu is a Lecturer with Australian Artificial intelligence Institute (AAII), University of Technology Sydney, Australia. He received his Ph.D. degree in computer science from AAII, University of Technology Sydney, Australia, in 2020. He received a M.Sc. degree in probability and statistics and a B.Sc. degree in pure mathematics from the School of Mathematics and Statistics, Lanzhou University, China, in 2015 and 2013, respectively. His research interests include machine learning and hypothesis testing. He has served as a senior program committee member for ECAI and program committee members for NeurIPS, ICML, ICLR, AISTATS, ACML, IJCAI, AAAI and so on. He also serves as reviewers for MLJ, TPAMI, TNNLS and TFS. He has received ICLR outstanding reviewer award (2021), Best paper award from AAII, UTS (2020), the UTS-FEIT HDR Research Excellence Award (2019), Best Student Paper Award of FUZZ-IEEE (2019) and UTS Research Publication Award (2018).

Zhen Fang received his M.Sc. degree in pure mathematics from the School of Mathematical Sciences Xiamen University, Xiamen, China, in 2017. He is working toward a PhD degree with the Faculty of Engineering and Information Technology, University of Technology Sydney, Australia. His research interests include transfer learning and domain adaptation. He is a Member of the Decision Systems and e-Service Intelligence (DeSI) Research Laboratory, AAII, University of Technology Sydney.

Bo Yuan received the B.E. degree from Nanjing University of Science and Technology, P.R. China, in 1998, and the M.Sc. and Ph.D. degrees from The University of Queensland (UQ), Australia, in 2002 and 2006, respectively, all in Computer Science. From 2006 to 2007, he was a Research Officer on a project funded by the Australian Research Council at UQ. He is currently an Associate Professor in the Division of Informatics, Shenzhen International Graduate School, Tsinghua University, P.R. China. He is the author of more than 110 papers in refereed international conferences and journals. His research interests include data science, evolutionary computation and reinforcement learning.

Guangquan Zhang is an Associate Professor and Director of the Decision Systems and e-Service Intelligent (DeSI) Research Laboratory with the Australian Artificial Intelligence Institute, University of Technology Sydney, Australia. He received a Ph.D. degree in applied mathematics from Curtin University of Technology, Australia, in 2001. His research interests include fuzzy modeling in machine learning and data analytics. He has authored five monographs, five textbooks, and 470 papers, including 225 refereed international journal papers. He has been awarded 9 Australian Research Council (ARC) Discovery Project and many other research grants. He was awarded an ARC QEII Fellowship in 2005. He has served in editorial boards of several international journals, and as a guest editor of eight special issues for IEEE Transactions and other international journals.

Jie Lu (F'18) is a Distinguished Professor and the Director of the Australian Artificial Intelligence Institute at the University of Technology Sydney, Australia. She is an IEEE Fellow, an IFSA Fellow and Australian Laureate Fellow. She received her PhD degree from the Curtin University, Australia, in 2000. Her main research expertise is in fuzzy transfer learning, decision support systems, concept drift and recommender systems. She has published six research books and 450 papers in IEEE Transactions and other journals and conferences. She has completed over 20 Australian Research Council discovery grants and other research projects. She serves as Editor-In-Chief for Knowledge-Based Systems (Elsevier) and Editor-In-Chief for the International Journal on Computational Intelligence Systems (Atlantis), has delivered 25 keynote speeches at international conferences, and has chaired 10 international conferences.